Journal of Photochemistry and Photobiology A: Chemistry 212 (2010) 27–35

Contents lists available at ScienceDirect

Journal of Photochemistry and Photobiology A: Chemistry

journal homepage: www.elsevier.com/locate/jphotochem

Photophysical study of a covalently linked quantum dot–low symmetry phthalocyanine conjugate

Wadzanai Chidawanyika, Christian Litwinski, Edith Antunes, Tebello Nyokong*

Department of Chemistry, Rhodes University, P.O. Box 94, Grahamstown 6140, South Africa

ARTICLE INFO

Article history:
Received 3 January 2010
Received in revised form 1 March 2010
Accepted 17 March 2010
Available online 27 March 2010

Keywords:
Quantum dots
Low symmetry phthalocyanine
Fluorescence lifetime
Förster resonance energy transfer
Triplet quantum yield
Triplet lifetime
Singlet oxygen

ABSTRACT

The linkage of a low symmetry phthalocyanine, ZnttbIPc to mercaptopropionic acid (MPA) capped CdTe quantum dots has been achieved using a coupling agent, dicyclohexylcarbodiimide (DCC), to facilitate formation of an amide bond. UV–vis, Raman and IR spectroscopic studies on the linked (QD:ZnttbIPc-linked) conjugate suggest the reaction was a success. Förster resonance energy transfer (FRET) resulted in stimulated emission of ZnttbIPc in both the linked (QD:ZnttbIPc-linked) and mixed (QD:ZnttbIPc-mixed) conjugates. The linked complex (QD:ZnttbIPc-linked) gave the largest FRET efficiency hence showing the advantages of covalent linking. Photophysicochemical properties of the phthalocyanine were improved in the presence of the QDs i.e. for QD:ZnttbIPc-mixed. Fluorescence lifetimes of QDs were unchanged in QD:ZnttbIPc-mixed and decreased for QD:ZnttbIPc-linked.

1. Introduction

Quantum dos (QDs) are a unique class of nanoparticles which have sparked widespread scientific research of late [1–5]. Their size dependent electronic properties are the most attractive features of these semiconductor nanocrystals [3]. Among these properties are their high fluorescence quantum yields, high photostability, narrow (tunable) emission spectra and broad-band excitation spectra [1–8].

QDs have found particular importance in medicinal applications [6,8–13] as nanoparticulate imaging probes. In most cases they have been conjugated to biologically active compounds such as proteins or site specific molecules.

Photodynamic therapy (PDT) is an emerging cancer treatment method, which makes use of the interaction between light and a photosensitizing agent to initiate cell (cancer) death [14,15]. Metallophthalocyanines (MPcs) are a robust group of molecules with suitable photochemical and photophysical properties and have shown potential as photosenstizers for PDT due to their intense red light absorption, non-toxicity, selective localization within tumours, singlet oxygen generation capabilities and excellent photostability [14–17]. Their chemical properties can be altered or tuned through modification of the phthalocyanine ring periphery with a variety of substituents [14,18,19]. However the limited solubility of these molecules in aqueous environments inhibits their use as sensitizers in the body particularly with respect to cell penetration. Nanoparticles, such as QDs are particularly useful in this respect as they have potential for use as delivery systems [20].

QDs have also been found to have the ability to transfer energy as donors to accepting molecules such as phthalocyanines [8,9,21–24]. This process is known as Förster resonance energy transfer (FRET), a non-radiative energy transfer process that occurs from a fluorescent donor to a suitable acceptor fluorophore in close proximity [8,12,25–27].

There has been limited research on chemically linked conjugates of QDs and phthalocyanines [28,29]. The reported linking has been through the axial ligand of the phthalocyanine [28] or using symmetrically tetrasubstituted tetraamino phthalocyanine [29], which does not give specificity since the number of linking points are unknown. The linking of QDs to low symmetry phthalocyanines is not known and is reported in this work for the first time. In this work we have linked mercaptopropionic acid (MPA) capped CdTe QDs to a previously synthesized low symmetry phthalocyanine: tris[9 (10),16 (17),23 (24)-tert-butyl]imidophthalocyaninato] zinc (II) (ZnttbIPc), Scheme 1, [30,31], using dicyclohexylcarbodiimide (DCC) as a coupling agent to facilitate formation of an amide bond between the carboxylic acid end of the QDs and the imide grouping of ZnttbIPc. The use of ZnttbIPc ensures only one linking point of QDs to the Pc. An investigation on the influence of the quan-

* Corresponding author. Tel.: +27 46 6038260; fax: +27 46 6225109.
E-mail address: t.nyokong@ru.ac.za (T. Nyokong).

1010-6030/$ – see front matter © 2010 Elsevier B.V. All rights reserved.
doi:10.1016/j.jphotochem.2010.03.008

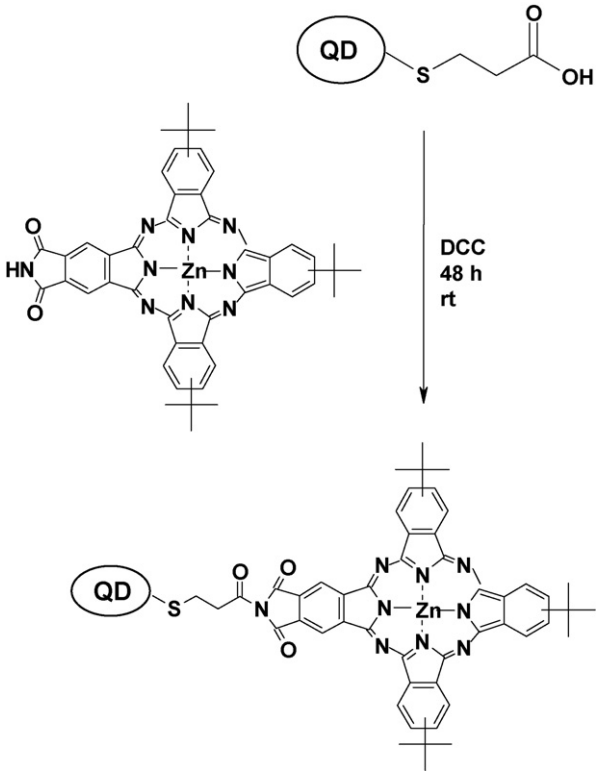

Scheme 1. Synthetic route to QD:ZnttblPc-linked conjugate.

tum dots on the photophysical properties of the low symmetry phthalocyanine has been conducted.

2. Experimental

2.1. Materials

$CdCl_2{\cdot}2H_2O$, dicylcohexylcarbodiimide (DCC), tellurium powder (200 mesh), 3-mercaptopropionic acid and Rhodamine 6G were purchased from Sigma–Aldrich. N,N-dimethylformamide (DMF), ethanol (EtOH), sodium azide, sodium borohydride and sodium hydroxide were obtained from SAARCHEM. Ultra pure water was obtained from a Milli-Q Water System (Millipore Corp., Bedford, MA, USA). A 4:1 (v/v) DMF:water solution was employed for all studies. This solvent mixture allows for solubilization of the quantum dots and phthalocyanine while maintaining the monomeric nature of the phthalocyanine.

2.2. Instrumentation

FTIR spectra (KBr pellets) were recorded on a Perkin-Elmer spectrum 2000 FTIR spectrometer. UV–vis (ultraviolet–visible) absorption spectra were recorded on a Cary 500 UV–vis–NIR spectrophotometer.

X-ray powder diffraction patterns were recorded on a Bruker D8, Discover equipped with a proportional counter, using Cu Kα radiation ($\lambda = 1.5405$ Å, nickel filter). Data were collected in the range from $2\theta = 15^\circ$ to 60°, scanning at $1^\circ\ min^{-1}$ with a filter time-constant of 2.5 s per step and a slit width of 6.0 mm. Samples were placed on a silicon wafer slide. The X-ray diffraction data were treated using the freely-available Eva (evaluation curve fitting) software. Baseline correction was performed on each diffraction pattern by subtracting a spline fitted to the curved background and the full width at half maximum values used in this study were obtained from the fitted curves.

Raman spectral data were collected with Bruker Vertex 70 – Ram II spectrometer (equipped with a 1064 nm Nd:YAG laser and a liquid nitrogen cooled germanium detector). Solid samples containing KBr were employed. Fluorescence emission and excitation spectra were obtained using a Varian Eclipse spectrofluorimeter. Fluorescence lifetimes were measured using a time correlated single photon counting set-up (TCSPC) (FluoTime 200, Picoquant GmbH).

The excitation sources were a light emitting diode (LED, PLS-500, 497 nm, 10 MHz repetition rate, Picoquant GmbH) with a linear polariser and a diode laser (LDH-P-C-485, 480 nm, 10 MHz repetition rate, Picoquant GmbH).

Fluorescence was detected under the magic angle with a peltier cooled photomultiplier tube (PMT) (PMA-C 192-N-M, Picoquant) and integrated electronics (PicoHarp 300E, Picoquant GmbH). A monochromator with a spectral width of 16 nm for the LED and 4 nm for the diode laser was used to select the required emission wavelength band. The response function of the system, which was measured with a scattering Ludox solution (DuPont), had a full width at half-maximum (FWHM) of about 950 ps for the LED and 300 ps for the diode laser. All luminescence decay curves were measured at the maximum of the emission peak and the lifetimes obtained by deconvolution of the decay curves using the FluoFit Software program (PicoQuant GmbH, Germany). The support plane approach [32] was used to estimate the errors of the decay times.

A laser flash photolysis system was used for the determination of triplet decay kinetics. The excitation pulses were produced by a Quanta-Ray Nd:YAG laser (1.5 J/9 ns), pumping a Lambda Physik FL 3002 dye laser (Pyridin 1 in methanol). The analyzing beam source was from a Thermo Oriel 66902 xenon arc lamp, and a Kratos Lis Projekte MLIS-X3 photomultiplier tube was used as the detector. Signals were recorded with a two-channel, 300 MHz digital real-time oscilloscope (Tektronix TDS 3032C); the kinetic curves were averaged over 256 laser pulses.

Singlet oxygen ($^1O_2$) luminescence at 1270 nm was measured with a system that was similar to an earlier reported method [33]. The set-up consists of an ultrasensitive Germanium detector (Edinburgh Instruments, EI-P) combined with a 1000 nm long pass filter (Omega, 3RD 1000 CP) and a 1270 nm band pass filter (Omega, C1275, BP50). Laser pulses were generated by the laser system described above. The near-infrared emission of the sample was focused to the detector by a lens (Edmund, NT 48-157) with a detection direction perpendicular to the excitation laser beam. The detected signals were averaged over 256 laser pulses, with the same oscilloscope described above, to show the dynamic decay of $^1O_2$. Direct comparison of the intensity corresponding to the 1270 nm signal for each sample with a reference (ZnPc in DMF) with a known singlet oxygen quantum yield ($\Phi_\Delta = 0.56$ [34]) allowed determination of singlet oxygen quantum yields.

2.3. Syntheses of CdTe MPA QDs

Thiol capped CdTe quantum dots were prepared by an aqueous hydrothermal method adapted from the literature [35–37]. A Cd precursor solution was prepared by dissolving $CdCl_2{\cdot}2H_2O$ (2.19 g, 10 mmol) in millipore water (110 mL) in a 3-necked flask. Mercaptocarboxylic acid (MPA) (2.55 g, 24 mmol) used as a capping agent for the CdTe QDs, was then added under stirring at room temperature. The solution was then adjusted to pH 12 by dropwise addition of 1 M NaOH and nitrogen gas bubbled through the solution for 1 h. The aqueous solution was then reacted with a NaHTe solution. The typical molar ratio of Cd:Te:Thiol in each experiment was 2:1:4.8. The NaHTe solution was prepared separately by a method described in the literature [35,38–40], with some modification. Briefly, 500 mg (13.2 mmol) of $NaBH_4$ was transferred to a 15 mL 3-neck flask, 10 mL of millipore water was added and nitrogen bubbled through the solution. Tellurium powder (640 mg) was

added to the flask after which an ice bath was maintained around the reaction flask for cooling. A small outlet was connected to the flask during the reaction to discharge the pressure from the resulting hydrogen. After ~8 h, the black tellurium powder disappeared and a white sodium tetraborate precipitate appeared at the bottom of the flask. The resulting clear supernatant contained NaHTe and this was separated and used in the preparation of the required CdTe particles. The freshly prepared oxygen-free NaHTe solution was injected into the Cd precursor solution under vigorous stirring. A rapid change in color occurred at this stage. The solution was then refluxed under air at 100 °C for different time periods to control the size of the CdTe QDs. Aliquots of the reaction solution were taken out at regular intervals and the fluorescence emission spectra recorded until the desired wavelength (and hence size) was achieved. Precipitation of the respective QDs from the aqueous solution was achieved using excess EtOH, following which the solutions were centrifuged to obtain solid QD samples which were dried in vacuo. The QD sizes were estimated using a polynomial fitting function (Eq. (1)) [41]:

$$D = (9.8127 \times 10^{-7})\lambda^3 - (1.7147 \times 10^{-3})\lambda^2 + (1.0064)\lambda - 194.84 \quad (1)$$

where λ refers to the absorption maxima of the QDs. This fitting function is not valid for sizes of quantum dots outside the size range of 1–9 nm [41]. The particle-diameter d, was also estimated using XRD. Solution concentrations of the QDs were calculated according to the literature methods [41].

2.4. Linking of ZnttbIPc to CdTe MPA QDs

The synthesis and characterization of ZnttbIPc has been reported elsewhere [30].

MPA capped CdTe QDs (7.5 mg) were first dissolved in water (1 mL), then DMF (4 mL) was added, followed by addition of DCC (3.28 mg, 0.016 mmol). The latter is used to convert the –COOH group of the QDs capping into an active carbodiimide ester group. The mixture was left to stir at room temperature under an argon atmosphere for 24 h. Thereafter, ZnttbIPc (0.13 mg, 1.56×10^{-4} mmol) was added to the reaction mixture and then left for another 48 h. The solid product was extracted and washed several times with DMF (to remove excess unreacted complex ZnttbIPc and any DCC intermediate by-products) and also washed with water to remove unlinked QDs. The washings were continued until the supernatants were clear, giving QD:ZnttbIPc-linked. IR [(KBr) υ_{max}/cm^{-1}]: 1645 ($\upsilon_{C=O}$). Experiments were also performed where the QDs were mixed with ZnttbIPc without linking, giving QD:ZnttbIPc-mixed, keeping the molar ratio of QDs to ZnttbIPc the same as for the linked. Experiments were also performed where molar ratios of QDs to ZnttbIPc were changed for the mixed system in order to determine the nature of QD quenching by ZnttbIPc.

2.5. Photochemical and photophysical parameters

2.5.1. Fluorescence studies

Fluorescence quantum yields (Φ_F) were determined by the comparative method [42] (Eq. (2)):

$$\Phi_F = \Phi_{F(Std)} \frac{F \cdot A_{Std} \cdot n^2}{F_{Std} \cdot A \cdot n_{Std}^2} \quad (2)$$

where F and F_{Std} refer to the integrated fluorescence intensity of the MPc and the reference respectively. A and A_{Std} are the absorbances of the sample and reference at the excitation wavelength respectively and n and n_{Std} are the refractive indices of solvents used for the sample and reference, respectively. For fluorescence quantum yield determinations of the ZnPc derivative ($\Phi_{F(ZnPc)}$) in the DMF:water (4:1) solvent mixture, ZnPc in DMF (Φ_F = 0.30 [43]) was used as a standard. Rhodamine 6G in ethanol (Φ_F = 0.94 [32,44]) was employed as a standard for the determination of the fluorescence quantum yields of the quantum dots ($\Phi_{F(QD)}$) in the DMF:water solvent mixture. Both the sample and reference were excited at the same wavelength.

The fluorescence quantum yields of the quantum dots are represented as $\Phi_{F(QD)}$ where QD represents CdTe MPA QDs and $\Phi_{F(ZnPc)}$ represents the quantum yield of the ZnttbIPc species. The quantum yield values determined for the quantum dots were employed in the determination of their fluorescence quantum yields in the mixture (QD:ZnttbIPc-mixed, $\Phi_{F(QD)}^{Mix}$) and in the linked form (QD:ZnttbIPc-linked, $\Phi_{F(QD)}^{Linked}$) using Eq. (3):

$$\Phi_{F(QD)}^{Mix} = \Phi_{F(QD)} \frac{F_{QD}^{Mix}}{F_{QD}} \quad (3a)$$

$$\Phi_{F(QD)}^{Linked} = \Phi_{F(QD)} \frac{F_{QD}^{Linked}}{F_{QD}} \quad (3b)$$

where $\Phi_{F(QD)}$ represents the fluorescence quantum yield of the QDs alone, and was used as a standard, F_{QD}^{Mix} or F_{QD}^{Linked} are the fluorescence intensities of QDs in the mixture with ZnttbIPc (QD:ZnttbIPc-mixed) or in the linked form (QD:ZnttbIPc-linked), respectively, when excited at the excitation wavelength of the QDs (510 nm) and F_{QD} is the fluorescence intensity of the QD alone at the same excitation wavelength.

Fluorescence lifetimes were obtained by deconvolution of the decay curves, obtained by time correlated single photon counting (TCSPC), using the FluoFit Software program (PicoQuant GmbH, Germany).

2.5.2. Triplet quantum yields and lifetimes

For triplet determinations, de-aerated solutions of the respective MPc complexes were introduced into a 1 cm pathlength spectrophotometric cell and irradiated at the Q-band with the laser system described above. Triplet quantum yields (Φ_T) of the MPc complexes were determined by the triplet absorption method. A comparative method, based on triplet decay [45] using ZnPc as standard, was employed for the calculations, Eq. (4):

$$\Phi_T = \Phi_T^{Std} \frac{\Delta A_T \cdot \varepsilon_T^{Std}}{\Delta A_T^{Std} \cdot \varepsilon_T} \quad (4)$$

where ΔA_T and ΔA_T^{Std} are the changes in the triplet state absorbances of the MPc derivative and the standard respectively; ε_T and ε_T^{Std}, the triplet state molar extinction coefficients for the MPc derivative and the standard respectively; Φ_T^{Std}, the triplet quantum yield for the standard (Φ_T^{Std} = 0.58 for ZnPc in DMF [46]).

At least three independent measurements of Φ_T, Φ_F and Φ_Δ were carried out, giving the errors shown in Tables.

Triplet lifetimes (τ_T) were determined by exponential fitting of the kinetic curves using OriginPro 7.5 software. The triplet quantum yield and lifetime of ZnttbIPc in the mixture or linked were also determined and are represented as $\Phi_{T(ZnPc)}^{Mix}$ (or $\Phi_{T(ZnPc)}^{Linked}$) and $\tau_{T(ZnPc)}^{Mix}$ (or $\tau_{T(ZnPc)}^{Linked}$), respectively.

Quantum yields of internal conversion (Φ_{IC}) were obtained from Eq. (5), which assumes that only three intrinsic processes (fluorescence, intersystem crossing and internal conversion); jointly deactivate the excited singlet state of an MPc molecule:

$$\Phi_{IC} = 1 - (\Phi_F + \Phi_T) \quad (5)$$

2.5.3. Singlet oxygen quantum yields

Singlet oxygen quantum yield values (Φ_Δ) values were determined in air by direct detection of the 1270 nm emission of singlet

oxygen using the equipment described above. Determinations were made in the absence and presence of sodium azide (NaN_3), a physical quencher of singlet oxygen.

The dynamic course of $^1O_2$ concentration [$^1O_2$] can be clearly recorded, following Eq. (6) as theoretically described in the literature [47]:

$$I = A\frac{\tau_D}{\tau_T - \tau_D}[e^{-t/\tau_T} - e^{-t/\tau_D}] \quad (6)$$

where, I is the luminescence intensity of $^1O_2$ at time t, τ_D is the lifetime of $^1O_2$ decay, τ_T is the ZnPc derivative triplet state lifetime and A is a coefficient involved in sensitizer concentration and $^1O_2$ quantum yield.

$^1O_2$ quantum yields (Φ_Δ of ZnttbIPc) were then determined using Eq. (7):

$$\Phi_\Delta = \Phi_\Delta^{Std} \cdot \frac{A \cdot OD^{Std}}{A^{Std} \cdot OD} \quad (7)$$

where Φ_Δ^{Std} is the singlet oxygen quantum yield for the standard ZnPc ($\Phi_\Delta^{Std} = 0.58$ for ZnPc in DMF [34]). A and A^{Std} refer to coefficient involved in sensitizer concentration and $^1O_2$ quantum yield for the sample and standard respectively and; OD and OD^{Std} to the optical density of the sample and standard respectively at the excitation wavelength.

Singlet oxygen quantum yields for the mixed were also determined using the same equations and are represented as $\Phi_{\Delta(ZnPc)}^{Mix}$. The singlet oxygen quantum yield for the linked could not be determined due to the low concentration of ZnttbIPc present and thus the singlet oxygen luminescence signals fell below the current detection limit.

2.5.4. Determination of FRET parameters

Förster resonance energy transfer (FRET) refers to the energy transfer process that can occur from a photoexcited donor fluorophore to an acceptor fluorophore of a different form, which is in close proximity. The donor molecules typically emit at shorter wavelengths which overlaps with the absorption spectrum of the acceptor. Energy transfer is a result of long-range dipole–dipole interactions between donor and acceptor. The rate of FRET is dependent on the center-to-center distance r between donor and acceptor, the extent of spectral overlap of the donor's emission spectrum and the acceptor's absorption spectrum, the emission quantum yield of the donor and the relative orientation of the donor and acceptor transition dipoles [25,32]. A decrease in the donor fluorescence emission accompanied by an increase in the acceptor's fluorescence is an indication that FRET has occurred.

The steady state FRET efficiency (Eff_{ss}) is determined experimentally from the fluorescence quantum yields of the donor in the absence ($\Phi_{F(QD)}$) and presence ($\Phi_{F(QD)}^{Mix}$ or $\Phi_{F(QD)}^{Linked}$) of the acceptor using Eq. (8) [25,32,48,49]:

$$Eff_{ss} = 1 - \frac{\Phi_{F(QD)}^{Mix}}{\Phi_{F(QD)}} \quad (8a)$$

$$Eff_{ss} = 1 - \frac{\Phi_{F(QD)}^{Linked}}{\Phi_{F(QD)}} \quad (8b)$$

The efficiency of energy transfer based on the fluorescence lifetimes (Eff_{tr}) was also computed from the lifetime measurements of the donor (QDs), in the absence (τ_D) and presence (τ_{DA}) of the acceptor (ZnttbIPc) using Eq. (9) [32,50]:

$$Eff_{tr} = 1 - \frac{\tau_{DA}}{\tau_D} \quad (9)$$

However, this equation makes the assumption that the decay of the donor is a single exponential in the absence (τ_D) and presence (τ_{DA}) of acceptor and thus holds rigorously only for a homogeneous system (i.e. identical donor–acceptor complexes) in which the donor and donor–acceptor complexes have single exponential decays [32]. Such single-exponential decays are rare in biomolecules. Thus for donor–acceptor systems decaying with multiexponential lifetimes the energy transfer efficiency must be calculated from the amplitude weighted lifetimes (Eq. (10)):

$$\tau_i = \sum\nolimits_i \alpha_i \tau_i \quad (10)$$

where α_i is the relative amplitude contribution to the lifetime τ. Therefore, in this case we have used the amplitude weighted time-constants for τ_D and τ_{DA} to determine the transfer efficiency, for the linked species (QD:ZnttbIPc-linked), using Eq. (9).

The FRET efficiency is related to r (Å), the donor–acceptor distance by Eq. (11) [32,51]:

$$Eff_{ss} = \frac{R_0^6}{R_0^6 + r^6} \quad (11)$$

where R_0 (the Förster distance, Å) is the critical distance between the donor and the acceptor molecules for which efficiency of energy transfer is 50% and depends on the quantum yield of the donor, Eq. (12) [32,51]:

$$R_0^6 = 8.8 \times 10^{23}\, \kappa^2 n^{-4} \Phi_{F(QD)} J \quad (12)$$

where κ^2 is the dipole orientation factor i.e. it describes the relative orientation of the transition dipoles of the donor and acceptor in space. In this case, it is assumed that κ^2 is 2/3. This assumption is often made for donor–acceptor pairs in a liquid medium, since their dipole moments are considered to be isotropically oriented during the excited state lifetimes. The use of the isotropic dynamical average ($\kappa^2 = 2/3$) is more appropriate than the static isotropic average ($\kappa^2 = 0.476$) because the donor–acceptor pair is not in a rigid medium. n is the refractive index of the solvent; $\Phi_{F(QD)}$, the fluorescence quantum yield of the donor in the absence of the acceptor; and J (cm^6) is the Förster overlap integral defined by Eq. (13):

$$J = \int f_{QD}(\lambda)\varepsilon_{ZnPc}(\lambda)\lambda^4 \partial\lambda \quad (13)$$

where f_{QD} is the normalized QD emission spectrum and ε_{ZnPc} is the molar extinction coefficient ($M^{-1}\,cm^{-1}$) of ZnttbIPc. λ is the wavelength (nm) of the acceptor i.e. the Q-band. FRET parameters were computed using the program PhotochemCAD [52].

3. Results and discussion

3.1. Syntheses and spectral characterization of quantum dots

Quantum dot synthesis was carried out following a well established literature method [35–40]. The optical tunability of quantum dots is related to their size and structural composition [8]. The growth kinetics associated with quantum dots are a result of the quantum confinement effect. With prolonged heating the quantum dots grow, a feature reflected by a red shift in their absorption and emission spectra. Termination of the growth process was carried out once the desired spectral overlap between the QD emission spectrum and absorption spectrum of ZnttbIPc was attained i.e. emission peak of 640 nm for CdTe MPA QDs used in this study (Fig. 1). The quantum dots are characterized by broad absorption peaks with tails extending into the near-infrared region.

CdTe QDs capped with thiols are known to aggregate in acid conditions due to detachment of surface ligands [53]. Aggregation of QDs results in red shifting in the emission spectra accompanied by broadening and decrease in the fluorescence lifetime [54]. Solvents also have an effect on the aggregation nature of CdTe QDs [54].

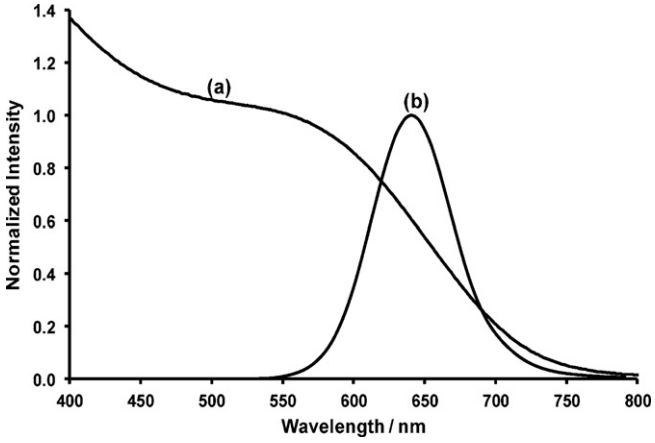

Fig. 1. (a) Normalized ground state electronic absorption and (b) emission spectra of CdTe MPA QDs (1 mg/mL in 4:1 (v/v) DMF:water, λ_{exc} = 510 nm).

There was no change in the emission spectrum of the QDs recorded from direct synthesis conditions in NaOH or when recorded using DMF:water mixture, Fig. 2A, showing that DMF has no effect on QDs. Also the fluorescence lifetime in NaOH or DMF:water mixture remained unchanged (Fig. 2B(i and ii), Table 1), confirming lack of aggregation on changing the solvent.

X-ray powder diffraction was used for particle size determination, Fig. 3. The diffraction pattern corresponds well with the three characteristic peaks for bulk CdTe structure.

The particle-diameter was generated by the computer software using the Scherrer equation (Eq. (14)):

$$d = \frac{k\lambda}{\beta \cos \theta} \tag{14}$$

where k corresponds to an empirical constant (0.9), λ is the X-ray source wavelength (1.5405 Å), β is the full width at half maximum of the diffraction peak and θ is the angle of the peak. XRD generated data related to the main peak at ~25° and gave a particle size of 3.41 nm. This size is slightly smaller but possibly more accurate in comparison to the size determined using the polynomial fitting function i.e. 3.50 nm.

Further studies with the developed QDs were carried out in a mixture with ZnttbIPc (QD:ZnttbIPc-mixed) and upon coupling of the QDs with ZnttbIPc using DCC (a coupling agent often used in organic solvents) to activate the carboxylic acid end of the thiol groups and thus give a linked conjugate (QD:ZnttbIPc-linked). In this case the carboxylic acid groups that terminate the MPA thiol groups used to passivate the QD surface were linked to the imide group of ZnttbIPc via an amide bond (Scheme 1). FTIR spectroscopy gave evidence of the formation of such a bond. A broad band at 1645 cm^{-1} that can be attributed to the carbonyl (C=O) stretch of the resultant amide bond was observed for the QD:ZnttbIPc-linked, Fig. 4A(d). Such a band was not observed in the CdTe MPA QDs alone (Fig. 4A(a)), ZnttbIPc alone (Fig. 4A(b)) or for QD:ZnttbIPc-mixed (Fig. 4A(c)). The regions of interest are indicated by a box in Fig. 4A.

In addition, Raman spectroscopy was employed to characterize the new complex, Fig. 4B. Again as was the case for FTIR, the regions of the Raman spectra that are of interest are indicated by a box in Fig. 4B. The main difference between the linked (QD:ZnttbIPc-linked, Fig. 4B(d)) and mixed (QD:ZnttbIPc-mixed, Fig. 4B(c)) conjugates was the position of the main peaks attributed to the phthalocyanine structure at 2851 and 2870 cm^{-1} respectively. The position of the 2870 cm^{-1} peak in ZnttbIPc alone (Fig. 4B(b)) is similar to that in QD:ZnttbIPc-mixed, suggesting minimal structural readjustment; however a shift of this peak for QD:ZnttbIPc-linked suggests the presence of a change in the molecular structure as a result of bond formation between the QDs and

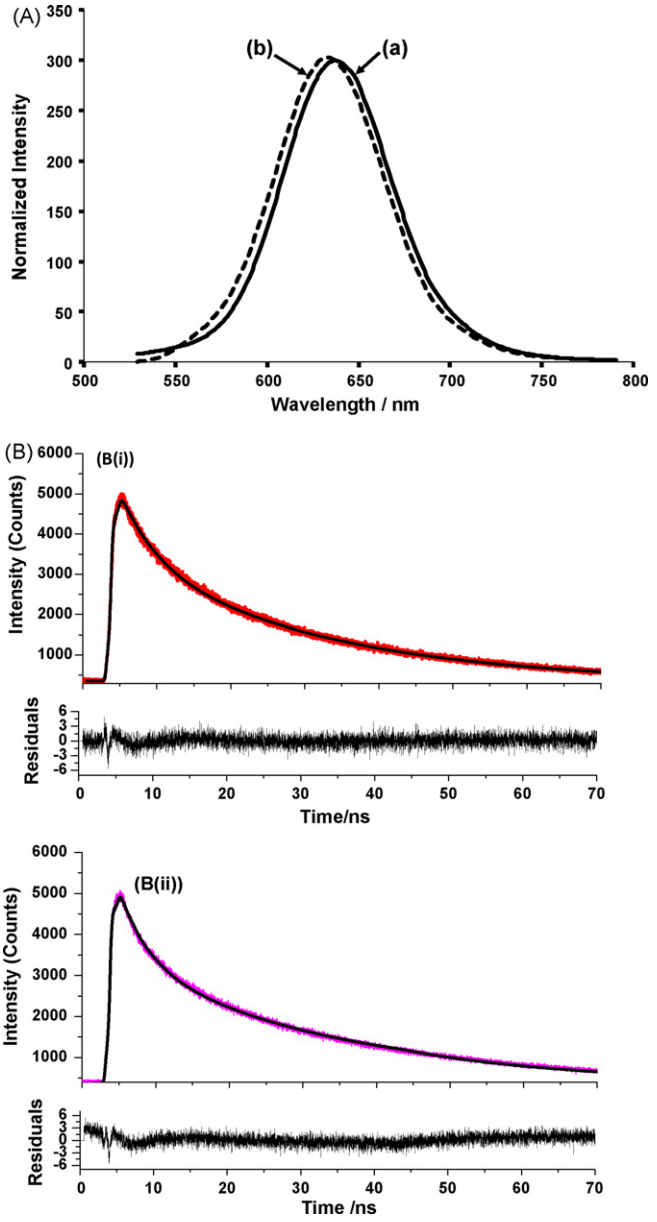

Fig. 2. (A) Comparison of emission spectra of QDs in (a) 0.1 M NaOH and (b) DMF:water (4:1) solvent mixture. (B) Photoluminescence decay curves of CdTe QDs in (i) 0.1 M NaOH solution and (ii) DMF:water (4:1) solvent mixture.

Table 1
TCSPC fluorescence data of QDs alone and QDs in QD:ZnttbIPc-mixed and QD:ZnttbIPc-linked obtained in DMF:water (4:1, v/v).

Compound	Relative A_1	$\tau_{F\text{-}1}$ (ns) (±0.5)	Relative A_2	$\tau_{F\text{-}2}$ (ns) (±0.3)
CdTe MPA QD	0.57 (0.61[a])	26.4 (26.3 [a])	0.43 (0.39 [a])	3.4 (4.3 [a])
QD:ZnttbIPc-mixed	0.57	28.6	0.43	3.2
QD:ZnttbIPc-linked	0.21	9.6	0.79	1.7

[a] Data obtained for CdTe MPA QDs alone in 0.1 M NaOH solution.

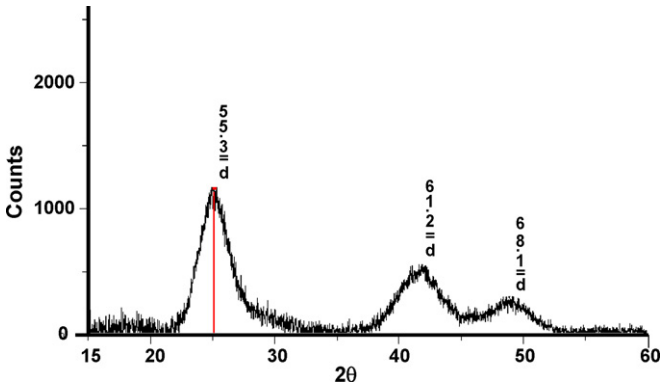

Fig. 3. X-ray diffractogram of mercaptopropionic acid stabilized CdTe quantum dots.

ZnttbIPc. Also apparent is the substantial decrease in intensity of the peak due to the QDs at ~3235 cm^{-1} (Fig. 4B(a)) in both the mixed and linked conjugates. The peaks at ~1600 cm^{-1} in both the QDs and ZnttbIPc also appear reduced in both conjugates.

Absorption spectra were used for further characterization of the mixed and linked species in the DMF:water solvent mixture (Fig. 5). This solvent mixture allows for solubilization of the quantum dots while maintaining the phthalocyanine in its monomeric form. A split (due to unsymmetrical nature of the complex) Q-band with peaks at 707 and 666 nm characteristic of ZnttbIPc [30,31] was observed. Interestingly there was a shift in the low energy component of the Q-band of QD:ZnttbIPc-mixed (Fig. 5c) towards higher energies (707–695 nm). This is indicative of non-specific binding of the MPcs onto the surface of QDs. No significant shift in the

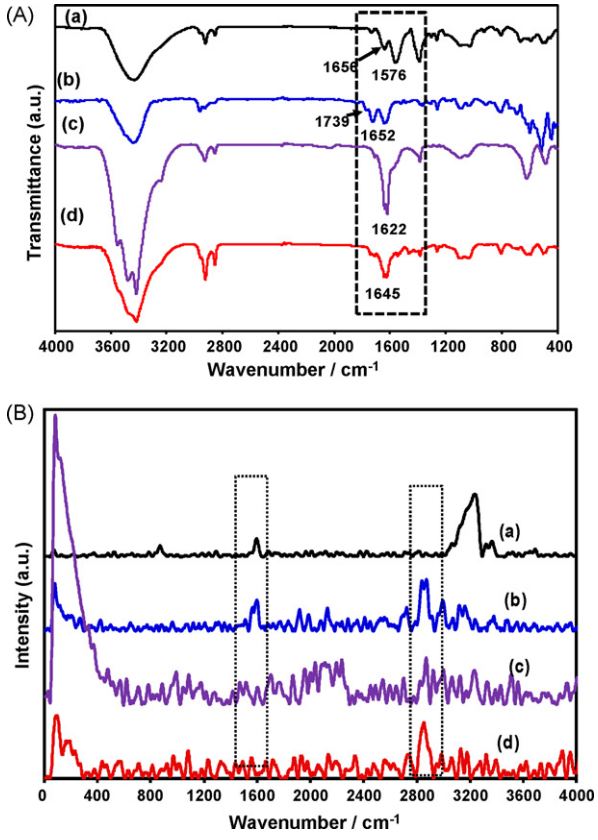

Fig. 4. (A) FTIR spectra of (a) CdTe MPA QDs alone, (b) ZnttbIPc alone, (c) QD:ZnttbIPc-mixed and (d) QD:ZnttbIPc-linked. (B) Raman spectra of (a) CdTe MPA QDs alone, (b) ZnttbIPc alone, (c) QD:ZnttbIPc-mixed and (d) QD:ZnttbIPc-linked.

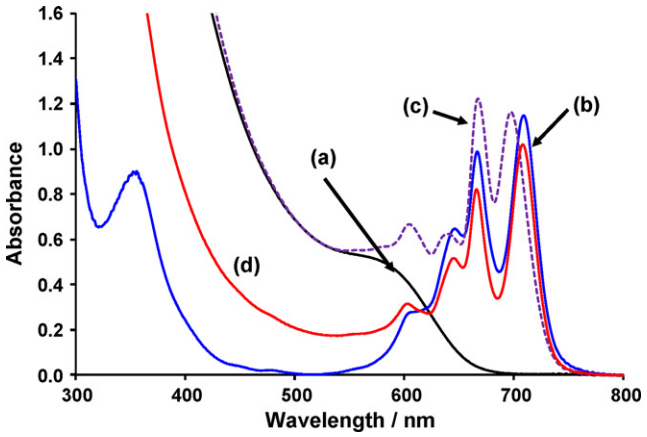

Fig. 5. Ground state electronic absorption spectra of (a) CdTe MPA QDs alone, (b) ZnttbIPc alone, (c) QD:ZnttbIPc-mixed and (d) QD:ZnttbIPc-linked in 4:1 (v/v) DMF:water solution.

Q-band of ZnttbIPc was observed on introduction of the QDs for the linked form. This difference in spectra between the linked and mixed is an indirect way of confirming the linkage. There was an increase in the absorption in the 500 nm region for QD:ZnttbIPc-linked and QD:ZnttbIPc-mixed due to the presence of QDs. The QD:ZnttbIPc-linked shows lower absorption in the 500 nm region than QD:ZnttbIPc-mixed, due to different amounts of QDs in the two. For the mixture (QD:ZnttbIPc-mixed), the interaction is probably in the form of adsorption.

Fluorescence in unsymmetrical phthalocyanine complexes such as ZnttbIPc occurs from the lowest energy vibrational band (ν_0) of S_1 (i.e. a transition from one energy level), resulting in one fluorescence peak [14,55] as shown in Fig. 6.

3.2. Fluorescence quantum yields and lifetimes

Fluorescence quantum yields ($\Phi_{F(QDs)}$) of CdTe MPA QDs were calculated using Eq. (2) and are in Table 2. The fluorescence quantum yields of QDs in the mixture (QD:ZnttbIPc-mixed) and linked forms (QD:ZnttbIPc-linked) are reduced relative to Φ_F values of the QDs alone, suggesting that the interaction with ZnttbIPc results in a quenching of the QD fluorescence. This is a regular occurrence for QDs in the presence of phthalocyanine units [8,9,22–24] and the quenching has been attributed to the transfer of energy from donor QDs to phthalocyanine acceptor molecules. This results in

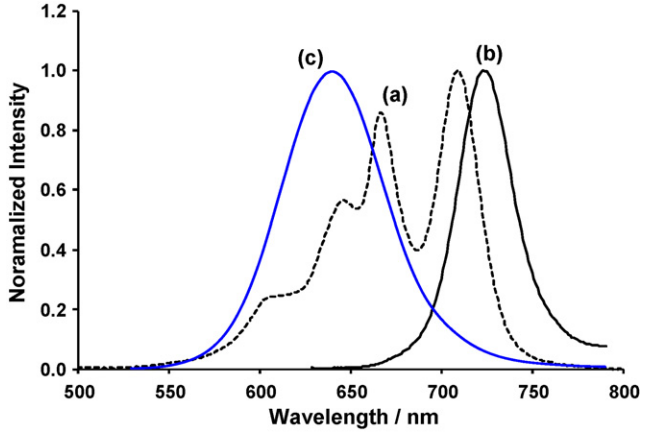

Fig. 6. Normalized (a) ground state absorption spectrum of ZnttbIPc and fluorescence emission spectra of (b) ZnttbIPc and (c) CdTe MPA QDs in 4:1 (v/v) DMF:water solution (λ_{exc} = 510 nm).

Table 2
Fluorescence quantum yields and photophysical parameters of ZnttbIPc in the presence of QDs in DMF:water (4:1, v/v).

Compound	$\Phi_{F(QD)}^{Mix/Linked}$ (±0.04) λ_{exc} = 510 nm	$\Phi_{T(ZnPc)}^{Mix/Linked}$ (±0.03) λ_{exc} = 666 nm	$\Phi_{\Delta(ZnPc)}^{Mix/Linked}$ (±0.01) λ_{exc} = 666 nm	$\Phi_{IC(ZnPc)}^{Mix/Linked}$	$\tau_{T(ZnPc)}^{Mix/Linked}$ (μs)
QD:ZnttbIPc-mixed	0.04 (0.09[a])	0.81 (0.77[b])	0.53 (0.45[b])	0.15 (0.15[b])	15 (70[b])
QD:ZnttbIPc-linked	0.02 (0.09[a])	0.73 (0.77[b])	0.48[c] (0.45[b])	0.26 (0.15[b])	48 (70[b])

[a] Φ_F of CdTe MPA QDs alone in DMF:water (4:1, v/v) are shown in brackets.
[b] Data pertaining to ZnttbIPc alone. Φ_F of ZnttbIPc alone = 0.08 in DMF:water.
[c] Value estimated as described in text.

a lowering of QD fluorescence intensity, in either a QD:ZnttbIPc-mixed or QD:ZnttbIPc-linked species, and therefore a reduction in fluorescence quantum yields of the QDs. Non-radiative (NR) decay processes may also be used to account for the decline in Φ_F values. The fluorescence quantum yield of ZnttbIPc ($\Phi_{F(ZnPc)}$) was calculated to be 0.08 which is the same as the value determined in DMF alone [31], hence showing no influence from the presence of water. The $\Phi_{F(ZnPc)}$ were not determined in the presence of QDs (linked or mixed), since excitation of the ZnttbIPc without exciting the QDs was not possible due to the broad absorption of the QDs.

Fluorescence lifetimes (τ_F) were determined for the QDs alone in NaOH and the 4:1 (v/v) DMF:water mixture as well as for the QD:ZnttbIPc-mixed and QD:ZnttbIPc-linked conjugates. The data obtained is shown in Table 1, which indicates that there is not much influence of a change in solvent with respect to the lifetimes (for the longer lifetimes in particular), of the QDs in NaOH ($\tau_{F\text{-}1}$ = 26.3 ns and $\tau_{F\text{-}2}$ = 4.3 ns) and DMF:water ($\tau_{F\text{-}1}$ = 26.4 ns and $\tau_{F\text{-}2}$ = 3.4 ns). The presence of biexponential decay kinetics is a common occurrence for QDs. Where, the literature suggests that the short lifetime component may be attributed to the intrinsic recombination of initially populated core states [56–58]. The origin of the longer lifetime component may be due to the involvement of surface states in the carrier recombination process [59]. The increase in radiative lifetime as a result of trapping of carrier states, by surface states, is a well established feature [57]. Therefore, it seems plausible that this may account for the data we have obtained, particularly since this long lifetime component is quenched to a larger degree on attachment of ZnttbIPc (Table 1). However, other researchers contradict this theory and suggest the faster decay component may rather be attributed to the surface states [50,60]. The difference in the short lifetime component that we obtained, under the influence of different solvents, may also support this theory, since a change in the solvent may exert more influence on the surface state properties of the QDs as opposed to the core. Therefore at this stage we cannot boldly make assignments with respect to the origin of the short and long lifetime components. Despite the quenching of the steady state fluorescence signal, there is not much change for the QD:ZnttbIPc-mixed conjugate ($\tau_{F\text{-}1}$ = 28.6 ns and $\tau_{F\text{-}2}$ = 3.2 ns), for which we expect slightly faster relaxation times. In this case, there may be numerous QD–Pc interactions, due to random distribution of donor–acceptor (QD–Pc) separations, owing to the lack of a formal bond. Hence, the presence of numerous acceptors (Pcs) at more than one distance results in more complex decays which cannot be resolved by our system [32,61]. As a result, the signal is dominated by the free QDs due to the poor interaction. However, the linked conjugate (QD:ZnttbIPc-linked), shows faster decay components which can be explained by the presence of a distinct bond between the QDs and Pc, which enable better interaction between the two and results in extensively quenched lifetimes (Table 1), which is a clear indication of energy transfer.

In order to evaluate the type of QD quenching by ZnttbIPc in QD:ZnttbIPc-mixed complexes, the time resolved fluorescence decay curves were recorded for different molar ratios of ZnttbIPc to mixed QDs, starting from 0.5:1 to 32:1 (Pc:QD), following the literature methods [62]. There was no change in the decay time with increase in the molar ratio of Pc:QDs, confirming static quenching of QD fluorescence by ZnttbIPc [32].

3.3. Förster resonance energy transfer (FRET) studies

The spectral overlap between the fluorescence emission of the QDs with the absorption spectrum of ZnttbIPc is shown in Fig. 6. The QDs in the mixture (QD:ZnttbIPc-mixed) and the linked form (QD:ZnttbIPc-linked) were excited at 510 nm, where ZnttbIPc does not absorb, and this resulted in a large decline of the QD fluorescence emission accompanied by stimulated fluorescence emission of ZnttbIPc at ~720 nm (Figs. 7b and 8b). This increase in fluorescence emission for ZnttbIPc in the presence of the MPA capped QDs implies transfer of energy, via FRET, from QDs to ZnttbIPc. Although there is stimulated emission for ZnttbIPc in the linked conjugate (QD:ZnttbIPc-linked), the extent of this emission is reduced in comparison to the mixed species. This may be attributed to the relative

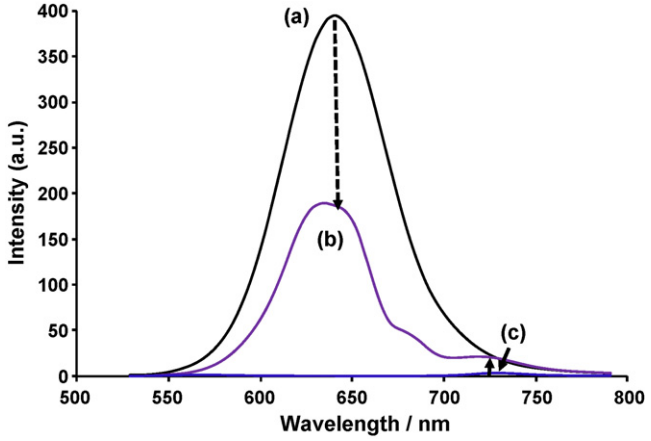

Fig. 7. Fluorescence emission spectra of (a) CdTe MPA QDs alone, (b) QD:ZnttbIPc-mixed and (c) ZnttbIPc alone in 4:1 (v/v) DMF:water solution (λ_{exc} = 510 nm).

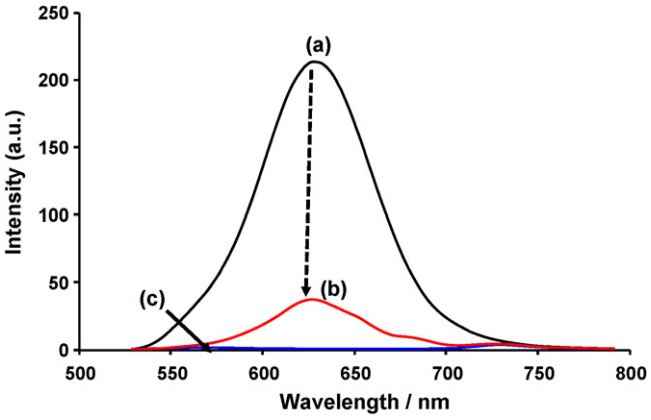

Fig. 8. (a) CdTe MPA QDs alone, (b) QD:ZnttbIPc-linked and (c) ZnttbIPc alone in 4:1 *v/v* DMF:water solution (λ_{exc} = 510 nm).

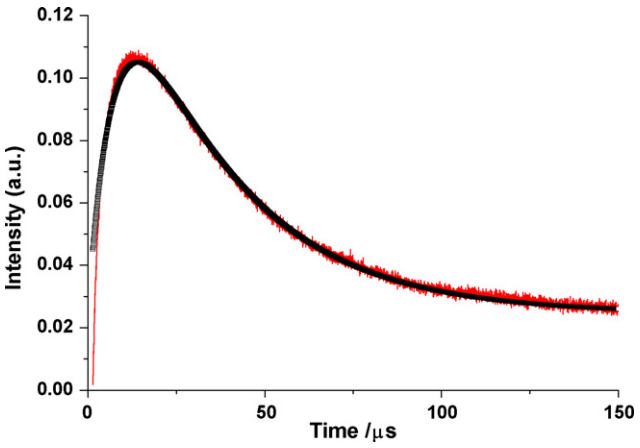

Fig. 9. $^1O_2$ decay curve (with fit) for ZnttbIPc DMF-water (4:1, v/v).

concentrations of ZnttbIPc and QDs present in solution. This makes any comparisons with the mixed species difficult. No significant emission was observed for ZnttbIPc alone on excitation at 510 nm (Figs. 8c and 9c). The presence of a second broad band at ~680 nm in the emission spectra of QDs, for both the mixed and linked conjugates may be attributed to exposure of surface defects at the QD surface which results in radiative recombination as a result of conjugation [12,63,64]. This may also contribute to the reduction in QD fluorescence intensity [65].

The efficiency with which FRET occurs is known to be dependent on several parameters, namely the spectral overlap (J), the value of which is shown in Table 3 is estimated by the overlap of the QD emission and ZnttbIPc absorption (Fig. 6). The value obtained for the mixed (QD:ZnttbIPc-mixed or linked) is quite large but lies within the expected range found for interactions with other phthalocyanine molecules [22–24]. A large J value is an indication of good spectral overlap and thus enhanced FRET efficiency. The Förster distance, R_0 (Å) is the critical distance between the donor and acceptor molecules for which energy transfer is 50% [51] is also shown in Table 3. The center-to-center separation distance, r (Å), between donor and acceptor were 44.08 and 34.70 Å, for the mixed and linked respectively. The steady state FRET efficiencies shown in Table 3 reflect relatively high transfer efficiencies i.e. 0.52 and 0.82 for the mixed and linked respectively. It appears that the large J values in combination with the small values of r result in ease of energy transfer and thus the high transfer efficiencies reflected in Table 3. The efficiency determined for QD:ZnttbIPc-mixed is lower than for QD:ZnttbIPc-linked. In the mixed conjugate, interactions between the QD and Pc occur only through Van der Waals interactions. Therefore energy transfer occurs only through space resulting in lower transfer efficiencies. Similar behavior has been observed for the interaction between SiPcs bearing methyl and tert-butyl axial ligands and CdSe QDs [28]. The higher efficiency determined for QD:ZnttbIPc-linked suggests the amide linkage brings the donor MPA capped QDs and the acceptor ZnttbIPc into closer proximity (smaller r than for QD:ZnttbIPc-mixed), resulting in better spectral overlap between the QD emission and Pc absorption and increased interaction, which thus facilitates better FRET. However it is also feasible that the FRET efficiency observed for the linked species also comprises non-radiative processes, due to the strong involvement of surface states that may deactivate the QD fluorophores. Thus the data obtained may not be a true reflection of FRET alone. Efficiencies determined, for QD:ZnttbIPc-linked, by steady state fluorescence and TCSPC, Eq. (9), were similar at 0.82 (by steady state fluorescence, Table 3) and 0.80 (by TCSPC), hence showing the compatibility of the two techniques.

Table 3
Energy transfer parameters for QD:ZnttbIPc-mixed and QD:ZnttbIPc-linked interactions in DMF:water (4:1, v/v).

Compound	J ($\times 10^{-13}$ cm^6)	R_0 ($\times 10^{-10}$ m)	r ($\times 10^{-10}$ m)	Eff_{ss}
QD:ZnttbIPc-mixed	6.40	44.68	44.08	0.52
QD:ZnttbIPc-linked	6.40	44.68	34.70	0.82

3.4. Triplet quantum yields (Φ_T) and lifetime (τ_T) studies

Triplet quantum yields (Φ_T) are determined to give a measure of the fraction of absorbing molecules that undergo intersystem crossing (ISC) to populate the triplet state (Φ_T). The triplet quantum yields of ZnttbIPc in the presence of QDs (mixed or linked) are shown in Table 2. An increase in Φ_T {from 0.77 (for ZbttbIPc alone) to 0.81 (for QD:ZnttbIPc-mixed)} was observed on introduction of the QDs. The increase is slight but significant within experimental error. The increase may be attributed to the presence of heavy Cd and Te atoms, which encourage ISC i.e. the heavy atom effect. The increase in triplet yield in the presence of QDs has been observed before [22–24]. QD:ZnttbIPc-linked gave a slightly lower yield of 0.73. This may be in relation to a lower ratio of phthalocyanine units to QDs as opposed to what may be present in the mixed species. The triplet lifetimes for the QD:ZnttbIPc-mixed decreased, Table 2, corresponding to the increase in the Φ_T value. The triplet lifetimes also decreased for the QD:ZnttbIPc-linked in Table 1.

There is an increase in Φ_{IC} value for QD:ZnttbIPc-linked (Φ_{IC} = 0.26) compared to that for ZnttbIPc alone (Φ_{IC} = 0.15), while for the mixed complex (QD:ZnttbIPc-mixed) there is no change in Φ_{IC} value (=0.15), this suggests that ZnttbIPc molecules become more deactivated through internal conversion as a result of linking to the CdTe MPA QDs.

3.5. Singlet oxygen quantum yields

Singlet oxygen quantum yields were determined using Eq. (7), with a decay curve shown in Fig. 9. Excitation was at 666 nm where ZnttbIPc absorbs. In the presence of CdTe MPA QDs (QD:ZnttbIPc-mixed) the singlet oxygen quantum yields were found to increase slightly, suggesting that the QDs enhance the transfer of energy from the triplet excited state of ZnttbIPc to ground state molecular O_2. In general, QDs alone do not produce significant amounts of $^1O_2$ (1%) [66]. However they exert some influence on the singlet oxygen generating capabilities of this ZnttbIPc. The efficiency of singlet oxygen generation is dependent on the amount of molecules that populate the triplet state i.e. triplet quantum yield (Φ_T) and their lifetime in this state (triplet lifetime, τ_T). High triplet yields and long lifetimes encourage increased molecular interactions between the triplet state of the photosensitizer (ZnttbIPc) and ground state oxygen resulting in higher singlet oxygen yields. Therefore the higher Φ_Δ for QD:ZnttbIPc-mixed relative to ZnttbIPc alone may be in response to higher population of the triplet state, as discussed above, from which energy is readily transferred to ground state molecular oxygen with high efficiency. The Φ_Δ value for the QD:ZnttbIPc-linked was not determined since the signal was very weak, most likely due to low concentrations of ZnttbIPc in the linked complex.

The efficiency of generation of singlet oxygen is represented by $S_\Delta = \Phi_\Delta/\Phi_T$ and the value for ZnttbIPc alone is S_Δ = 0.58 and that for the QD:ZnttbIPc-mixed is S_Δ = 0.65. Assuming that the efficiency of singlet oxygen generation does not change much between the linked and the mixed complexes, an estimated value of Φ_Δ = 0.48 for QD:ZnttbIPc-linked. This is a rough estimation, but it is reasonable since energy transfer efficiency is mainly dependent on MPc triplet state energy and the triplet excited state quantum yields and lifetime of the MPc.

4. Conclusions

Spectroscopic studies have been used to determine the successful linkage of CdTe MPA QDs to a low symmetry phthalocyanine, ZnttbIPc. Fluorescence spectra gave evidence of FRET in both the mixed and linked QD–Pc conjugates. The presence of QDs was found to improve the photophysicochemical properties of ZnttbIPc, with the mixed species, QD:ZnttbIPc-mixed giving favourable triplet quantum yields (Φ_T) and singlet oxygen quantum yields (Φ_Δ). The fluorescence lifetimes of the QDs in the mixed conjugate remained unchanged while that of QD:ZnttbIPc-linked showed faster decay times. The linked complex QD:ZnttbIPc-linked gave the largest FRET efficiency, hence showing that linking enhances FRET.

Acknowledgements

This work has been supported by the Department of Science and Technology (DST) and National Research Foundation (NRF), South Africa through DST/NRF Chairs Initiative for Professor of Medicinal Chemistry and Nanotechnology and Rhodes University. WC thanks the Andrew Mellon Foundation and NRF for scholarships.

References

[1] C. Seydel, Science 300 (2003) 80.
[2] J. Aldana, Y.A. Wang, X. Peng, J. Am. Chem. Soc. 123 (2001) 8844.
[3] L. Qu, X. Peng, J. Am. Chem. Soc. 124 (2002) 2049.
[4] A. Shavel, N. Gaponik, A. Eychmuller, J. Phys. Chem. B 110 (2006) 19280.
[5] H. Zhang, L. Wang, H. Xiong, L. Hu, B. Yang, W. Li, Adv. Mater. 15 (2003) 1712.
[6] W.C.W. Chan, S. Nie, Science 281 (1998) 2016.
[7] J.M. Haremza, M.A. Hahn, T.D. Krauss, Nano Lett. 11 (2002) 1253.
[8] A.C.S. Samia, X. Chen, C. Burda, J. Am. Chem. Soc. 125 (2003) 15736.
[9] S. Dayal, R. Krolicki, Y. Lou, X. Qiu, J.C. Berlin, M.E. Kenney, C. Burda, Appl. Phys. B 84 (2006) 309.
[10] M.E. Wieder, D.C. Hone, M.J. Cook, M.M. Handsley, J. Gavrilovic, D.A. Russell, Photochem. Photobiol. Sci. 5 (2006) 727.
[11] A.M. Smith, H. Duan, A.M. Mohs, S. Nie, Adv. Drug Deliv. Rev. 60 (2008) 1226.
[12] A.C.S. Samia, S. Dayal, C. Burda, Photochem. Photobiol. 82 (2006) 617.
[13] D.K. Chatterjee, L.S. Fong, Y. Zhang, Adv. Drug Deliv. Rev. 60 (2008) 1627.
[14] R. Bonnett, Chemical Aspects of Photodynamic Therapy, Gordon and Breach Science Publishers, Amsterdam, 2000.
[15] R.K. Pandey, J. Porphyr. Phthalocya. 4 (2000) 368.
[16] R.L. Morris, K. Azizuddin, M. Lam, J. Berlin, A. Nieminen, M.E. Kenney, A.C.S. Samia, C. Burda, N.L. Olenick, Cancer Res. 63 (2003) 5194.
[17] I.J. Macdonald, T.J. Dougherty, J. Porphyr. Phthalocya. 5 (2001) 105.
[18] C.M. Allen, W.M. Sharman, J.E. van Lier, J. Porphyr. Phthalocya. 5 (2001) 161.
[19] S McKeown F N.B., in The Porphyrin Handbook, K.M. Kadish, K.M. Smith, R.Guilard, (Eds.), vol. 15, Ch. 98, p. 61 (2003).
[20] I. Roy, T.Y. Ohulchanskyy, H.E. Pudavar, E.J. Bergey, A.R. Oseroff, J. Morgan, T.J. Dougherty, P.N. Prasad, J. Am. Chem. Soc. 125 (2003) 7860.
[21] S. Dayal, Y. Lou, A.C.S. Samia, J.C. Berlin, M.E. Kenney, C. Burda, J. Am. Chem. Soc. 128 (2006) 13974.
[22] M. Idowu, J.-Y. Chen, T. Nyokong, New J. Chem. 32 (2008) 290.
[23] S. Moeno, T. Nyokong, Polyhedron 27 (2008) 1953.
[24] S. Moeno, T. Nyokong, J. Photochem. Photobiol. A: Chem. 201 (2009) 228.
[25] L. Stryer, Annu. Rev. Biochem. 47 (1978) 819.
[26] S. Dayal, C. Burda, J. Am. Chem. Soc. 129 (2007) 7977.
[27] L. Lankiewicz, J. Malicka, W. Wizck, Acta Biochim. Polym. 44 (1997) 477.
[28] S. Dayal, J. Li, Y.-S. Li, H. Wu, A.C.S. Samia, M.E. Kenney, C. Burda, Photochem. Photobiol. 84 (2008) 243.
[29] J. Britton, E. Antunes, T. Nyokong, Inorg, Chem. Commun. 12 (2009) 828.
[30] W. Chidawanyika, J. Mack, S. Shimizu, N. Kobayashi, T. Nyokong, J. Porphyr. Phthalocya. 13 (2009) 1053.
[31] W. Chidawanyika, T. Nyokong, J. Photochem. Photobiol. A Chem. 206 (2009) 169.
[32] J.R. Lakowicz, Principles of Fluorescence Spectroscopy, 2nd ed., Kluwer Academic/Plenum Publishers, New York, 1999.
[33] M. Niedre, M.S. Patterson, B.C. Wilson, Photochem. Photobiol. 75 (2003) 382.
[34] W. Spiller, H. Kliesch, D. Worhle, S. Hackbarth, B. Roder, G. Schnurpfeil, J. Porphyr. Phthalocya. 2 (1998) 145.
[35] N. Gaponik, D.V. Talapin, A.L. Rogach, K. Hoppe, E.V. Shevchenko, A. Kornowski, A. Eychmüller, H. Weller, J. Phys. Chem. B 106 (2002) 7177.
[36] M.Y. Gao, S. Kirstein, H. Mohwald, A.L. Rogach, A. Kornokowski, A. Eychmüller, H. Weller, J. Phys. Chem. B 102 (1998) 8360.
[37] P. Zhong, Y. Yu, J. Wu, Y. Lai, B. Chen, Z. Long, C. Liang, Talanta 70 (2006) 902.
[38] H. Zhang, Z. Zhou, B. Yang, J. Phys. Chem. B 107 (2003) 8.
[39] D.L. Klayman, T.S. Griffin, J. Am. Chem. Soc. 95 (1973) 197.
[40] Z. Tang, N.A. Kotov, M. Giersig, Science 297 (2002) 237.
[41] W.W. Yu, L. Qu, W. Guo, X. Peng, Chem. Mater. 15 (2003) 2854.
[42] S. Fery-Forgues, D. Lavabre, J. Chem. Ed. 76 (1999) 1260.
[43] T. Shen, Z.-L. Yuan, H.-J. Xu, Dyes Pigment 11 (1989) 77.
[44] R.F. Kubin, A.N. Fletcher, J. Lumin. 27 (1982) 455.
[45] T.H. Tran-Thi, C. Desforge, C. Thiec, J. Phys. Chem. 93 (1989) 1226.
[46] J. Kossanyi, D. Chahraoui, Int. J. Photoenergy 2 (2000) 9.
[47] M.S. Patterson, S.J. Madsen, R. Wilson, J. Photochem, Photobiol. B: Biol. 5 (1990) 69.
[48] J.S. Hsiao, B.P. Krueger, R.W. Wagner, T.E. Johnson, J.K. Delaney, D.C. Mauzerall, G.R. Fleming, J.S. Lindsey, D.F. Bocian, R.J. Donohoe, J. Am. Chem. Soc. 118 (1996) 11181.
[49] P. Jacques, A.M. Braun, Helv. Chim. Acta 64 (1981) 1800.
[50] E.Z. Chong, D.R. Matthews, H.D. Summers, K.L. Njoh, R.J. Errington, P.J. Smith, J. Biomed. Biotechnol. 54169 (2007) 1.
[51] T. Förster, Discuss. Faraday Soc. 27 (1959) 7.
[52] H. Du, R.A. Fuh, J. Li, L.A. Cockan, J.S. Lindsey, Photochem. Photobiol. 68 (1998) 141.
[53] C. Bullen, P. Mulvaney, Langmuir 22 (2006) 3007.
[54] A. Mandal, N. Tamai, J. Phys. Chem. C 112 (2008) 8244.
[55] W. Freyer, S. Mueller, K. Teuchner, K.J. Photochem, Photobiol. A: Chem. 163 (2004) 231.
[56] M. Lunz, A. Louise Bradley, J. Phys. Chem. C 113 (2009) 3084.
[57] J. Zhang, X. Wang, M. Xiao, Opt. Lett. 27 (2002) 1253.
[58] M.G. Bawendi, P.J. Carroll, W.L. Wilson, L.E. Bruce, J. Chem. Phys. 96 (1992) 946.
[59] X. Wang, L. Qu, J. Zhang, X. Peng, M. Xiao, Nano Lett. 3 (2003) 1103.
[60] A. Javier, D. Magana, T. Jennings, G.F. Strouse, Appl. Phys. Lett. 83 (2003) 1423.
[61] L.V. Borkovska, L.P. Germash, N.O. Korsunska, E.Yu. Pecherska, Ukr. J. Phys. 53 (2008) 1002.
[62] A.R. Cortan, R. Hull, R.L. Opila, M.G. Bawendi, M.L. Steigerwald, R.J. Carroll, L.E. Brus, J. Am. Chem. Soc. 112 (1990) 1327.
[63] S. Sadhu, M. Tachiya, A. Patra, J. Phys. Chem. C 113 (2009) 19488.
[64] M. Kasha, H.R. Rawls, M. Ashraf El-Bayoumi, Pure Appl. Chem. 11 (1965) 371.
[65] Y.J. Hu, Y. Liu, R.M. Zhao, J.X. Dong, S.S. Qu, J. Photochem. Photobiol. A 179 (2006) 324.
[66] J. Ma, J.-Y. Chen, M. Idowu, T. Nyokong, J. Phys. Chem. B 112 (15) (2008) 4465–4469.